SCIENTIFIC REPORTS

OPEN

Estrogen deficiency impairs integrin $\alpha_v\beta_3$-mediated mechanosensation by osteocytes and alters osteoclastogenic paracrine signalling

Received: 3 December 2018
Accepted: 26 February 2019
Published online: 15 March 2019

Ivor P. Geoghegan[1,2], David A. Hoey[2,3,4,5] & Laoise M. McNamara[1,2]

The integrin $\alpha_v\beta_3$ has been shown to play an important role in osteocyte mechanotransduction. It has been reported that there are fewer β_3 integrin-containing cells in osteoporotic bone cells. Osteocytes cultured *in vitro* under estrogen deficient conditions demonstrate altered mechanotransduction. However, it is unknown whether the altered mechanotransduction in estrogen deficient osteocytes is directly associated with defective $\alpha_v\beta_3$ expression or signalling. The objective of this study is to investigate the role of estrogen deficiency for regulating MLO-Y4 cell morphology, $\alpha_v\beta_3$ expression, focal adhesion formation and mechanotransduction by osteocytes. Here, we report that estrogen withdrawal leads to a smaller focal adhesion area and reduced $\alpha_v\beta_3$ localisation at focal adhesion sites, resulting in an increased *Rankl/Opg* ratio and defective *Cox-2* responses to oscillatory fluid flow. Interestingly, $\alpha_v\beta_3$ antagonism had a similar effect on focal adhesion assembly, *Rankl/Opg* ratio, and *Cox-2* responses to oscillatory fluid flow. Taken together, our results provide the first evidence for a relationship between estrogen withdrawal and defective $\alpha_v\beta_3$-mediated signalling. Specifically, this study implicates estrogen withdrawal as a putative mechanism responsible for altered $\alpha_v\beta_3$ expression and resultant changes in downstream signalling in osteocytes during post-menopausal osteoporosis, which might provide an important, but previously unidentified, contribution to the bone loss cascade.

Osteocytes are the most abundant cells in bone and are responsible for mediating the balance between bone formation and resorption[1]. It has been proposed that osteocytes detect mechanical stimuli using mechanosensitive proteins, include stretch activated ion channels, gap junctions, primary cilia and integrins[2–4] and transduce them into biochemical responses[5,6]. Molecular factors produced by osteocytes regulate osteoclasts and osteoblasts, in particular RANKL and sclerostin, which promote osteoclast formation and inhibit osteoblastogenesis respectively, and OPG, which acts as a decoy receptor for RANK and thereby prevents osteoclast formation[7–10].

Integrins are heterodimeric transmembrane proteins, comprised of α and β subunits, which connect the intracellular cytoskeleton to the extracellular matrix through protein complexes known as focal adhesions (FA), which also comprise proteins such as vinculin, α-actinin, talin, and paxillin[11,12]. Focal adhesions are involved in Focal Adhesion Kinase (FAK) and shc signalling[13,14] and are widely understood to play a role in mechanosensation for many distinct cell types[15–21]. Osteocytes express both β_1 and β_3 integrins[4,11] and it has been shown that β_1 integrins localise around osteocyte cell bodies, whereas osteocyte cell processes have $\alpha_v\beta_3$ integrins and both interact with the surrounding pericellular matrix[4,22]. It has been proposed integrin based adhesions and pericellular matrix tethers together facilitate strain amplification[4,23–25]. *In vitro* studies have shown that Ca^{2+} response to a fluid

[1]Mechanobiology and Medical Device Research Group (MMDRG), Biomedical Engineering, National University of, Ireland, Galway, Ireland. [2]Centre for Research in Medical Devices (CÚRAM), National University of Ireland, Galway, Ireland. [3]Trinity Centre for Bioengineering, Trinity Biomedical Sciences Institute, Trinity College Dublin, Dublin 2, Ireland. [4]Department of Mechanical and Manufacturing Engineering, School of Engineering, Trinity College Dublin, Dublin 2, Ireland. [5]Advanced Materials and Bioengineering Research Centre, Trinity College Dublin & RCSI, Dublin 2, Ireland. Correspondence and requests for materials should be addressed to L.M.M. (email: Laoise.McNamara@nuigalway.ie)

stimulus was highly polarised along osteocyte cell processes but this Ca^{2+} response was compromised when cultured with a small molecule inhibitor of $\alpha_v\beta_3$[17]. Moreover, when $\alpha_v\beta_3$ was blocked using an antagonist, *Cox-2* expression and PGE_2 release were reduced and cell morphology was altered, whereby the cells had a reduced cell area and fewer cell processes[15].

Post-menopausal osteoporosis is a disease characterised by a decrease in circulating estrogen levels and an imbalance in bone cell remodelling, which causes bone loss and an increased susceptibility to fracture[26]. Estrogen acts as a regulator to maintain the balance of osteoblasts and osteoclasts[27] and enhances the response of bone cells to mechanical stress[28]. It has been reported that the estrogen receptors, ERα and ERβ, play a role in this mechanobiological response by osteoblasts and osteocytes[29,30]. In osteoblasts, estrogen was shown to increase *Opg* expression and augment *Cox-2* (via β_1 integrins and ERs) response to fluid shear stress[31,32] and decrease *Rankl* and *Sost* expression[33,34]. In osteocytes, supraphysiological levels of estrogen (100 nM) were shown to have a protective role against apoptosis[35,36], to induce an intracellular Ca^{2+} response[37] and increase connexion 43 gap junction expression and mechanosensitivity[38]. *In vitro* supplementation of culture media with levels of estrogen (10 nM) within the range of estrogen in healthy humans (pre-menopausal), was shown to led to increased osteogenic signalling by MLO-Y4 osteocytes[39]. However, most *in vitro* studies of osteocyte biology use culture media without exogenous estrogen, and thus there is a limited understanding of pre-menopausal levels of estrogen on osteocyte biology.

Human osteoblastic bone cells derived from osteoporotic patients have been shown to exhibit an impaired biochemical response (PGE_2) to mechanical stress compared to those derived from healthy patients[40]. Estrogen deficiency *in vitro* can be achieved by pre-treatment with 17β-estradiol followed by estrogen withdrawal or addition of an estrogen receptor antagonist[39,41]. Estrogen withdrawal in osteocytes was shown to attenuate fluid flow-induced intracellular calcium signalling, thus altering osteocyte mechanosensitivity[39], and lead to higher levels of osteocyte apoptosis, compared to estrogen treated cells[41]. Estrogen deficiency induced by ovariectomy (OVX) has been shown to lead to an altered tissue composition and mineral distribution within bone, altered mechanical environment of osteocytes and a reduction in β_3-positive cells in cortical bone compared to controls[42–44]. However, it is unknown whether such changes arise as a direct response to reduced estrogen or the ability of the β_3 integrins to facilitate mechanotransduction.

In this study, we test the hypothesis that altered osteocyte mechanosensitivity during estrogen deficiency is associated with an impairment in the mechanotransduction by β_3 integrins. Specifically, we investigate (1) the role of pre-menopausal levels of estrogen for regulating MLO-Y4 cell morphology, focal adhesion formation and mechanotransduction response to fluid flow, (2) changes in $\alpha_v\beta_3$ expression and spatial organisation in osteocytes during estrogen deficiency, and (3) whether altered mechanosensitivity of osteocytes under estrogen deficiency correlate to defective $\alpha_v\beta_3$ expression and functionality.

Results

Estrogen supplementation, to mimic pre-menopausal levels, leads to more mature FA assembly and actin cytoskeleton, and increased Opg expression compared to osteocytes cultured in standard media. *In vitro* studies of MLO-Y4 osteocyte biology commonly use α-MEM culture media without the addition of estrogen. However, *in vivo* estrogen is important for normal bone cell function and so, to more closely mimic the physiological environment of osteocytes *in vivo*, in this study we first investigated the effect of supplementing culture media with pre-menopausal levels of estrogen (10 nM) on MLO-Y4 osteocytes under static and oscillatory flow conditions *in vitro*.

A robust cytoskeleton with distinct focal adhesion sites can be seen in both control and estrogen treated cells under static culture conditions (Fig. 1A). Quantification of these images showed that estrogen supplementation leads to the development of larger cells ($p = 0.0525$), which have more focal adhesions ($p < 0.05$) and most interestingly, these cells also have a significantly larger focal adhesion area ($p < 0.01$) ($N = 3$, $n \geq 111$ cells per group), see Figs 1B,C and S1A. The actin fluorescence intensity was greater and the cells exhibited a higher degree of organisation (anisotropy) of the actin cytoskeleton in estrogen treated cells compared to controls ($p < 0.0001$ and $p < 0.0001$ respectively, $N = 3$, $n \geq 111$ cells per group) (Fig. 1D,E). Moreover, estrogen treated osteocytes were shown to express higher levels of *Opg* ($p < 0.01$, $n = 7–10$), but *Rankl* expression was unaffected, and this ultimately resulted in a lower *Rankl*/*Opg* ratio ($p = 0.0645$, $N = 5–7$) (Fig. 1F–H). There was no difference in *Cox-2* expression in the estrogen treated group compared to controls (Fig. 1I). Thus, estrogen supplementation leads to larger osteocytes with more mature FA assembly and a more robust actin cytoskeleton, and these changes are accompanied by a reduction in gene expression associated with osteoclast differentiation (*Rankl*/*Opg*).

The application of oscillatory fluid flow resulted in an increase in actin fluorescent intensity for both control and estrogen treated cells, when compared to their static counterparts ($p < 0.0001$ and $p < 0.01$ respectively, $N = 3$, $n \geq 111$ cells per group). However, fluid flow had no effect on cell area, focal adhesion area, or actin anisotropy for either cohort. Fluid shear stress led to a higher *Opg* expression in the control group ($p < 0.05$, $N = 7–10$), but had no effect on *Rankl* expression, and therefore, led to a lower *Rankl*/*Opg* ratio in that same group ($p = 0.051$, $N = 5–7$). There was no effect of fluid shear stress on *Rankl* or *Opg* expression in the estrogen treated group. Both control and estrogen treated cells showed a higher *Cox-2* response to fluid shear stress ($p < 0.05$ and $p < 0.05$ respectively, $N = 5–7$).

In summary, treatment of osteocytes *in vitro* with endogenous levels of estrogen, to mimic the pre-menopausal status of osteocyte biology, significantly alters cell behaviour, resulting in a more established cytoskeleton and a shift towards a more osteogenic phenotype when compared to widely used culture media for studies of MLO-Y4 osteocyte biology. Therefore, the estrogen treated groups were used as a control for studies of estrogen withdrawal, which are presented hereafter.

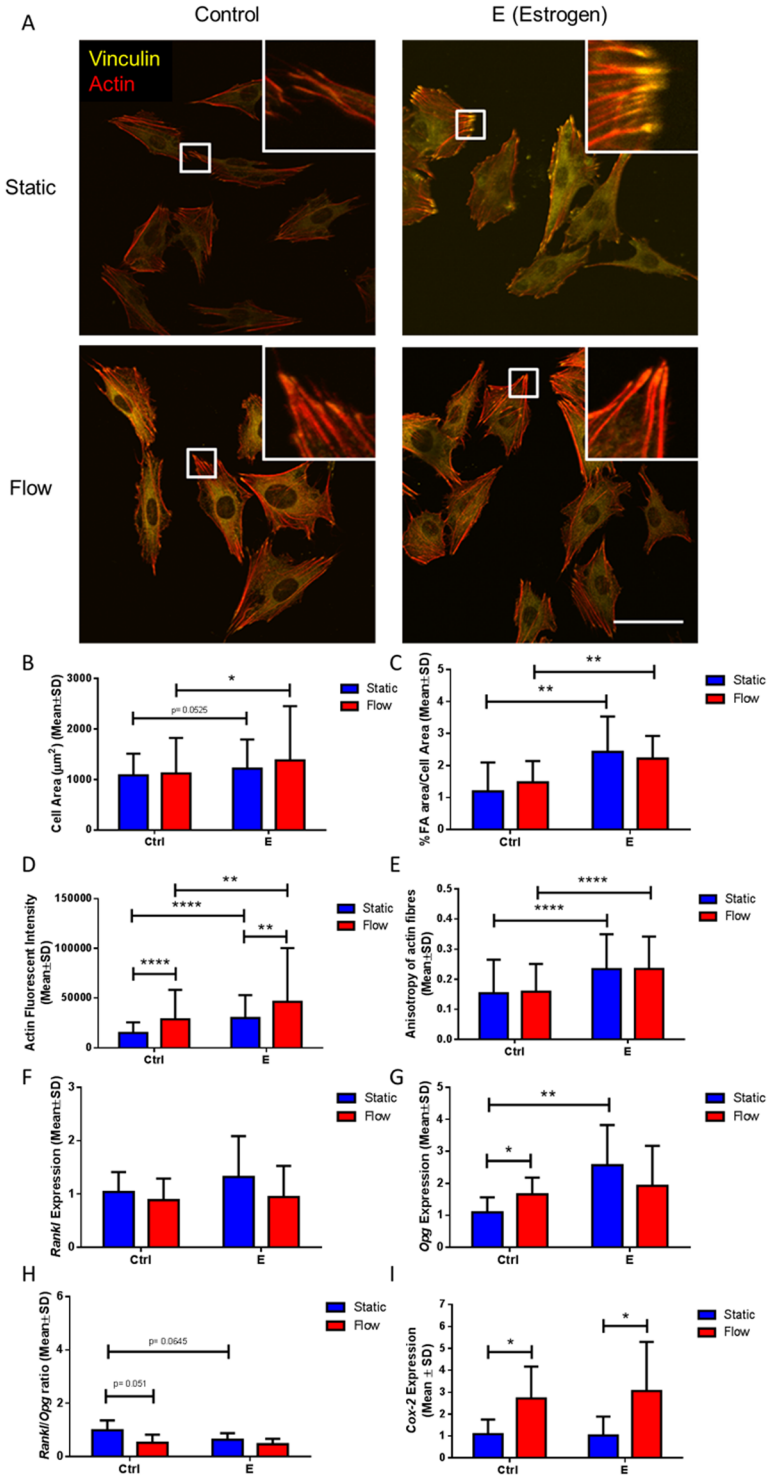

Figure 1. The effect of estrogen treatment and oscillatory fluid flow on MLO-Y4 cell morphology and downstream signalling. (**A**) Immunocytochemistry images showing actin fibres and vinculin staining (N = 3, n ≥ 111 cells per group). Quantification of the images showing (**B**) cell area, (**C**) % focal adhesion area/cell area, (**D**) actin fluorescent intensity, and (**E**) anisotropy of actin fibres. RT-PCR results of (F) *Rankl* expression (N = 5–10), (G) *Opg* expression (N = 7–10), (**H**) *Rankl*/*Opg* ratio (N = 5–7), and (I) *Cox-2* expression (N = 7–8) (Student's t-test, *p < 0.05, **p < 0.01, ****p < 0.0001).

Estrogen withdrawal alters osteocyte morphology, and this affect is further augmented by mechanical stimulation. Next we wished to understand what role estrogen withdrawal had on osteocyte morphology under both static and mechanical loading conditions.

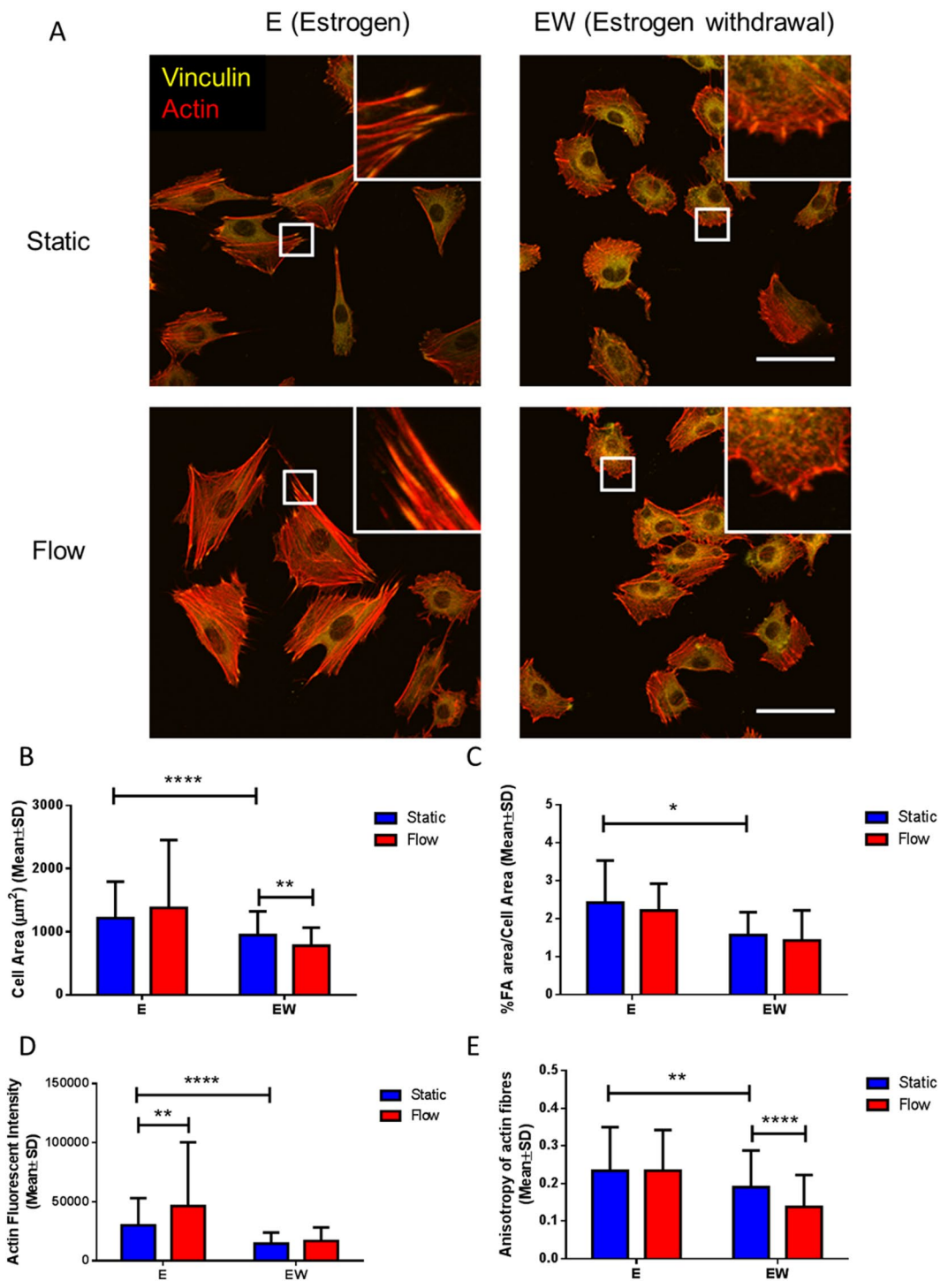

Figure 2. The effect of estrogen withdrawal and oscillatory fluid flow on MLO-Y4 cell morphology. (**A**) Immunocytochemistry images showing actin fibres and vinculin staining ($N = 3$, $n \geq 115$ cells per group). Quantification of the images showing (**B**) cell area, (**C**) % focal adhesion area/cell area, (**D**) actin fluorescent intensity and (**E**) anisotropy of actin fibres. (Student's t-test, *$p < 0.05$, **$p < 0.01$, ****$p < 0.0001$).

Under static conditions, cells cultured under estrogen withdrawal were observed to be smaller by immunostaining, and while they had focal adhesion sites, these were disordered, which was in contrast to estrogen treated cells that had distinct focal adhesion sites (Fig. 2A). Quantitative analysis of the actin and vinculin staining confirmed that cells cultured under estrogen withdrawal had a reduced cell and focal adhesion area, when compared to cells cultured under continuous estrogen conditions ($p < 0.0001$ and $p < 0.05$ respectively, $N = 3$, $n \geq 115$ cells per group) (Fig. 2B,C). The actin staining in the estrogen withdrawal cells was less intense and there were fewer stress fibres, when compared to the estrogen treated cells, which had noticeable and numerous stress fibres

(Fig. 2A). Quantitative analysis of the actin staining confirmed that the intensity and anisotropy of the actin fibres were lower following estrogen withdrawal in comparison to estrogen conditions ($p < 0.0001$ and $p < 0.01$ respectively, $N = 3$, $n \geq 115$ cells per group) (Fig. 2D,E), demonstrating a less robust and ordered actin cytoskeleton for estrogen deficient osteocytes under static conditions.

Fluid shear stress led to a lower cell area in estrogen withdrawal cells when compared to its static counterpart ($p < 0.01$, $N = 3$, $n \geq 115$ cells per group), but there was no difference in cell area or focal adhesion area following flow in the estrogen supplemented cells. Oscillatory fluid flow led to more intense actin staining in estrogen cells, compared to static groups ($p < 0.01$, $N = 3$, $n \geq 115$ cells per group), but this was not observed for estrogen withdrawal cells, which also exhibited had a lower anisotropy following fluid flow ($p < 0.0001$, $N = 3$, $n \geq 115$ cells per group), indicating a less ordered actin fibre organisation. Taken together, this data points to a defect in the formation of mechanosensitive focal adhesion sites following estrogen withdrawal.

Estrogen withdrawal resulted in reduced $\alpha_v\beta_3$ localisation at focal adhesion sites. Given the perturbed focal adhesion assembly seen in estrogen withdrawal conditions, we next investigated the effect of estrogen withdrawal on $\alpha_v\beta_3$ quantity and organisation. ELISA measurements of total $\alpha_v\beta_3$ content within MLO-Y4 cells showed no statistical differences following estrogen withdrawal ($p = 0.0612$, $N = 6$) (Fig. 3B). However, analysis of immunocytochemistry imaging showed significantly lower $\alpha_v\beta_3$ intensity per cell in estrogen withdrawal cells, compared to estrogen supplemented cells ($p < 0.05$, $N = 3$, $n \geq 115$ cells per group) (Fig. 3C). At focal adhesion (FA) sites, this lowered $\alpha_v\beta_3$ intensity in estrogen withdrawal cells was even more pronounced ($p < 0.01$, $N = 3$, $n \geq 115$ cells per group) (Fig. 3D). A less ordered $\alpha_v\beta_3$ organisation at FA sites was also qualitatively seen in the immunocytochemistry images for estrogen withdrawal osteocytes (Fig. 3A).

The application of oscillatory fluid flow led to higher $\alpha_v\beta_3$ content in both estrogen and estrogen withdrawal groups compared to their static counterparts ($p < 0.01$ and $p < 0.05$ respectively, $N = 6$). This relationship was also seen in the $\alpha_v\beta_3$ intensity across the whole cell area ($p < 0.01$ and $p < 0.0001$ respectively, $N = 3$, $n \geq 115$ cells per group), but not at FA sites. Overall, these results demonstrate that estrogen withdrawal led to a lower $\alpha_v\beta_3$ quantity and impaired organisation at a cell-level and, more importantly, at mechanosensitive focal adhesion sites.

Estrogen withdrawal upregulated expression of genes associated with paracrine osteoclastogenic signalling (Rankl/Opg ratio), but perturbed the Cox-2 response to fluid shear stress. Given the alterations in MLO-Y4 cell morphology and $\alpha_v\beta_3$ organisation during estrogen withdrawal, we next investigated the effect of estrogen deficiency on genes associated with mechanotransduction (*Cox-2*) and osteoclastogenesis (*Rankl* and *Opg*). Under static culture conditions, estrogen withdrawal led to an upregulation in *Rankl* expression, in comparison to cells cultured under continuous estrogen culture, ($p = 0.0587$, $N = 7–8$), as well as a significant downregulation in *Opg* expression ($p < 0.05$, $N = 8–9$) (Fig. 4A,B). This resulted in a higher *Rankl*/*Opg* ratio in estrogen withdrawal conditions in comparison to the E group ($p < 0.05$, $N = 5–7$) (Fig. 4C).

After application of oscillatory fluid flow, Rankl expression was lower in the estrogen withdrawal group, compared to its static counterpart ($p < 0.05$, $N = 7–8$). However, there was no noticeable effect of flow on *Opg* expression, and ultimately there was no significant difference in the *Rankl*/*Opg* ratio for cells that underwent estrogen withdrawal and were mechanically stimulated (Fig. 4A–C).

For cells cultured under static conditions, estrogen withdrawal had no significant effect on *Cox-2* expression, when compared to the estrogen supplemented cells (Fig. 4D). The application of fluid shear stress led to a higher *Cox-2* response in the estrogen supplemented group, when compared to its static counterpart ($p < 0.05$, $N = 7–8$). However, this response to fluid flow was lost in estrogen withdrawal cells.

Taken together, these results demonstrate that estrogen withdrawal perturbed the normal osteogenic responses to mechanical stimulation by osteocytes, and also lead to the alteration in genes associated with paracrine osteoclastogenic signalling.

$\alpha_v\beta_3$ antagonism led to an altered cell morphology, as seen with estrogen withdrawal. Due to the fact that we showed a disorganised $\alpha_v\beta_3$ organisation under estrogen withdrawal conditions, we wished to investigate whether the perturbed cell function and responses to flow following estrogen withdrawal were associated with an altered $\alpha_v\beta_3$ function. Therefore, we used a small molecular inhibitor to block $\alpha_v\beta_3$ function.

Osteocytes that underwent $\alpha_v\beta_3$ antagonism demonstrated a perturbed morphology, with a visually smaller cell area and fewer distinct focal adhesion sites visible in the estrogen group (Fig. 5A), in comparison to unblocked counterparts, see Fig. 2A. Quantification of the images confirmed a lower cell area ($p < 0.0001$), focal adhesion area ($p < 0.01$), and focal adhesion number ($p < 0.05$) in the estrogen cells following $\alpha_v\beta_3$ antagonism ($N = 3$, $n \geq 90$ cells per group) (Figs 5B,C and S1C). However, there was no statistical difference in cell area, focal adhesion area or number between blocked and unblocked cells in the estrogen withdrawn cells. Actin was also shown to be affected by $\alpha_v\beta_3$ antagonism; whereby there was a lower actin fluorescent intensity and anisotropy in estrogen supplemented cells following $\alpha_v\beta_3$ antagonism ($p < 0.01$, $p < 0.0001$, $p < 0.0001$ and $p < 0.0001$ respectively, $N = 3$, $n \geq 90$ cells per group) (Fig. 5D,E). In estrogen withdrawal cells, $\alpha_v\beta_3$ antagonism led to lower actin intensity in cells subjected to oscillatory fluid flow, and a lower actin anisotropy between the static groups ($p < 0.0001$ and $p < 0.001$ respectively, $N = 3$, $n \geq 90$ cells per group).

A key finding was that the estrogen cells that underwent $\alpha_v\beta_3$ antagonism showed a similar morphology to the estrogen withdrawal cells (unblocked). Quantitative analysis of the images confirmed no difference in cell area, focal adhesion area, or actin cytoskeleton intensity and organisation between estrogen cells following $\alpha_v\beta_3$ antagonism and estrogen withdrawal cells (unblocked). These results clearly underpin the importance of $\alpha_v\beta_3$ on overall cell function and implicate the dysregulation of the integrin $\alpha_v\beta_3$ for the impaired cell morphology during estrogen withdrawal.

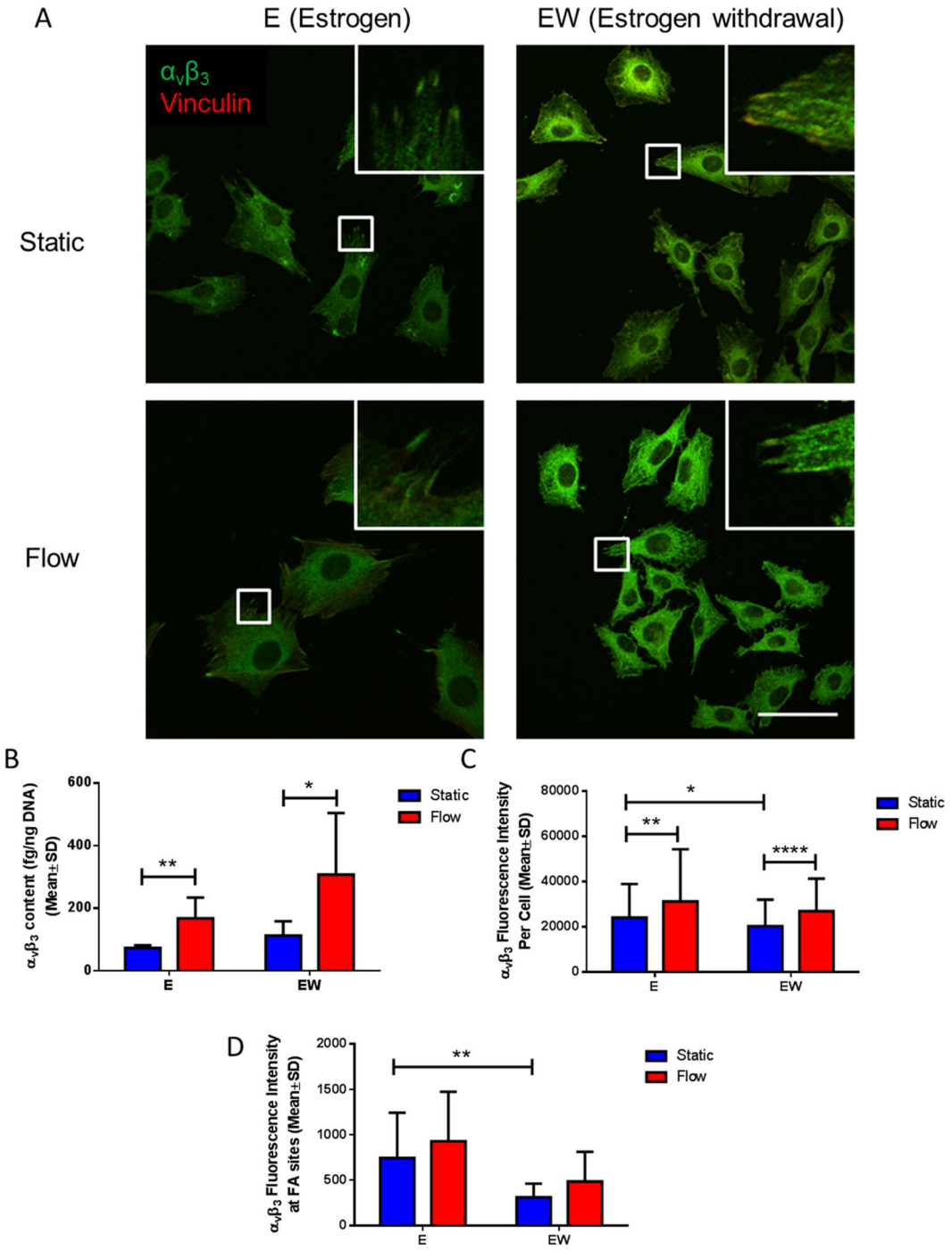

Figure 3. The effect of estrogen withdrawal and oscillatory fluid flow on $\alpha_v\beta_3$ quantity and organisation in MLO-Y4 cells. (**A**) Immunocytochemistry images showing $\alpha_v\beta_3$ and vinculin staining ($N = 3$, $n \geq 115$ cells per group). (**B**) ELISA measurement of total $\alpha_v\beta_3$ quantity normalised to DNA content ($N = 6$). Quantification of the images showing (**C**) $\alpha_v\beta_3$ intensity per cell, and (**D**) $\alpha_v\beta_3$ intensity at focal adhesion (FA) sites (Student's t-test, $^*p < 0.05$, $^{**}p < 0.01$, $^{****}p < 0.0001$).

$\alpha_v\beta_3$ antagonism led to a lower $\alpha_v\beta_3$ intensity per cell and at FA sites. To confirm the efficacy of the $\alpha_v\beta_3$ antagonism, we investigated the $\alpha_v\beta_3$ quantity following antagonism. We investigated the intensity of $\alpha_v\beta_3$ per cell and at FA sites using immunostaining. As expected, we saw a lower $\alpha_v\beta_3$ intensity per cell and at FA sites in the estrogen cells in comparison to their unblocked counterparts ($p < 0.05$, $p < 0.0001$, $p < 0.01$, and $p < 0.05$ respectively, $N = 3$, $n \geq 90$ cells per group) (Fig. 6C,D). In the estrogen withdrawal groups, we saw no change in $\alpha_v\beta_3$ intensity per cell and at FA sites following antagonism, indicating that the estrogen withdrawal groups already had a lowered $\alpha_v\beta_3$ quantity prior to antagonism. Further to this, there was no statistical difference in the intensity of $\alpha_v\beta_3$ between $\alpha_v\beta_3$ blocked estrogen cells and unblocked estrogen withdrawal cells. These

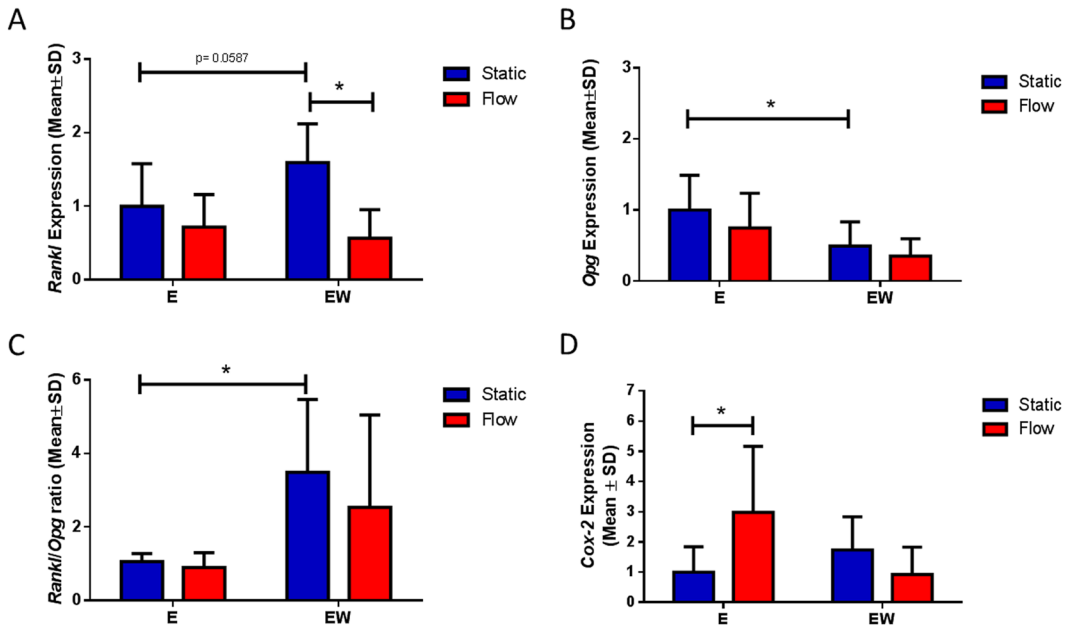

Figure 4. The effect of estrogen withdrawal and oscillatory fluid flow on osteoclastogenic and osteogenic signalling. RT-PCR results of (**A**) *Rankl* expression (N = 7–8), (**B**) *Opg* expression (N = 8–9), (**C**) *Rankl*/*Opg* ratio (N = 5–7), and (**D**) *Cox-2* expression (N = 7–8) (Student's t-test, *$p < 0.05$).

results further confirm that estrogen withdrawal has a negative effect on $\alpha_v\beta_3$ integrin quantity and organisation. ELISA measurements of $\alpha_v\beta_3$ antagonism showed a higher $\alpha_v\beta_3$ content compared to unblocked counterparts ($p < 0.05$, $p < 0.05$ and $p < 0.05$ respectively, N = 6) (Fig. 6B).

$\alpha_v\beta_3$ antagonism affected the Rankl/Opg response to estrogen withdrawal and resulted in a perturbed Cox-2 response to fluid flow. Finally, we wished to delineate the role of the integrin $\alpha_v\beta_3$ in the altered *Rankl*/*Opg* and *Cox-2* responses, seen during estrogen withdrawal. $\alpha_v\beta_3$ antagonism attenuated the higher *Rankl* response and lower *Opg* response seen previously in estrogen withdrawal conditions (Fig. 7A,B) and in turn resulted in no change in *Rankl*/*Opg* ratio in estrogen withdrawal cells (Fig. 7C). This lack of *Rankl*/*Opg* response to the estrogen withdrawal conditions following antagonism may implicate the integrin $\alpha_v\beta_3$ as an important transducer of estrogen-related signalling. Moreover, following $\alpha_v\beta_3$ antagonism, the *Cox-2* response to flow was absent in all groups (Fig. 7D). Taken together, these results show the importance of changes in the localisation of the integrin $\alpha_v\beta_3$ in the estrogen deficient conditions of post-menopausal osteoporosis.

Discussion

Given the importance of the integrin $\alpha_v\beta_3$ in osteocyte mechanotransduction, we sought to investigate the effect of estrogen withdrawal on the integrin $\alpha_v\beta_3$ and $\alpha_v\beta_3$-mediated signalling. Here, we report for the first time that, under static conditions, cell area, focal adhesion area, and the distribution of $\alpha_v\beta_3$ at mechanosensitive focal adhesion sites were all negatively affected by estrogen withdrawal conditions. Moreover, downstream mechanotransduction signalling associated with the integrin $\alpha_v\beta_3$ (*Cox-2* gene expression) was negatively affected following estrogen withdrawal. Osteocytes, in static conditions, that underwent estrogen withdrawal also increased expression of the *Rankl* gene and downregulated *Opg* expression, which are known to regulate osteoclastogenesis in a paracrine fashion. To investigate whether the integrin $\alpha_v\beta_3$ was responsible for the changes seen in estrogen withdrawal conditions, we blocked the integrin $\alpha_v\beta_3$ with an antagonist. Most interestingly, we report similar changes in cell morphology and downstream signalling in the absence of functional $\alpha_v\beta_3$ mechanoreceptors, as we had observed for cells that underwent estrogen withdrawal. Therefore, our results implicate a link between the estrogen withdrawal conditions of post-menopausal osteoporosis and altered $\alpha_v\beta_3$ functionality (Fig. 8).

Previous studies have clearly demonstrated defective osteocyte mechanotransduction during estrogen withdrawal *in vitro*[39,42]. *In vivo*, the number of β_3-containing bone cells in cortical bone was lower compared to controls in an estrogen deficient rat model of post-menopausal osteoporosis[42]. Here, we demonstrate an altered osteocyte morphology, specifically by means of a lower cell area and altered actin cytoskeleton, following estrogen withdrawal, which is in keeping with previous research[39]. We report for the first time impaired focal adhesion assembly in cells that are cultured under estrogen withdrawal conditions, along with a lower $\alpha_v\beta_3$ intensity at these compromised focal adhesion sites. Disperse cytosolic staining of vinculin was clearly visible in estrogen withdrawal cells. However, only distinct focal adhesion sites were quantified. The $\alpha_v\beta_3$ staining in our estrogen treated cells showed similarities to studies of MLO-Y4 cells in culture media (without estrogen supplementation)[15,45], but the spatial relationship of $\alpha_v\beta_3$ to other FA proteins, such as vinculin, has not been previously investigated. Recently, β_3 integrins were found along mouse osteocyte cells processes *in vivo* within specialised structures containing pannexin1, P2X7R, and CaV3.2-1. However, in that study the larger vinculin containing-focal adhesion complexes were found around the cell body and not the tightly packed cell processes, due to space constraints[22].

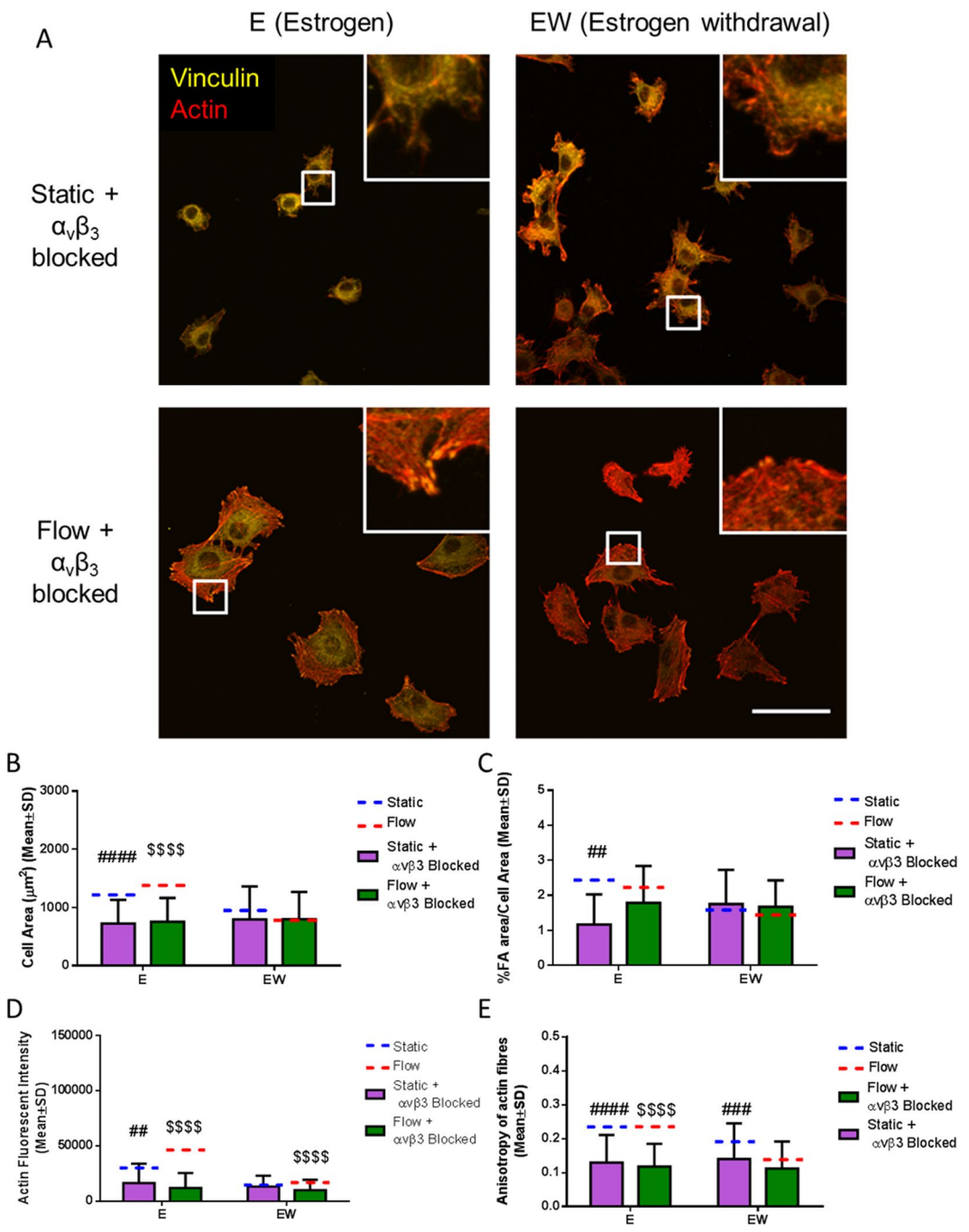

Figure 5. The effect of $\alpha_v\beta_3$ antagonism and oscillatory fluid flow on MLO-Y4 cell morphology. (**A**) Immunocytochemistry images showing actin fibres and vinculin staining ($N = 3$, $n \geq 90$ cells per group). Quantification of the images showing (**B**) cell area, (**C**) % focal adhesion area/cell area, (**D**) actin fluorescent intensity, and (**E**) anisotropy of actin fibres. (Student's t-test, $^{\#\#}p < 0.01$ compared to static, $^{\#\#\#}p < 0.001$ compared to static, $^{\#\#\#\#}p < 0.0001$ compared to static, $^{\$\$\$\$}p < 0.0001$ compared to flow).

In our *in vitro* study, cells do not have space constraints, and we show that vinculin co-localises with $\alpha_v\beta_3$ integrin. While it is known that the β_3 integrin binding sites along osteocyte cell processes are key sites in osteocyte mechanotransduction *in vivo*, particularly due to strain amplification, computational modelling has shown that osteocytes subjected to fluid shear stress *in vitro*, as seen in in this study, do transduce this mechanical stimulation through integrin binding sites found along the cell processes and cell body[46]. As such, we have measured focal adhesion sites found along the cell processes and cell body in our study.

Together our findings of an increase in *Rankl*/*Opg* ratio, under static conditions, and abrogation of the *Cox-2* response to oscillatory fluid flow demonstrate an altered response to mechanical stimulation in estrogen withdrawal conditions. RANKL is a cytokine produced by osteocytes, which binds to RANK receptors on osteoclast progenitors and regulates osteoclast differentiation and activity, whereas OPG is also produced by osteocytes but

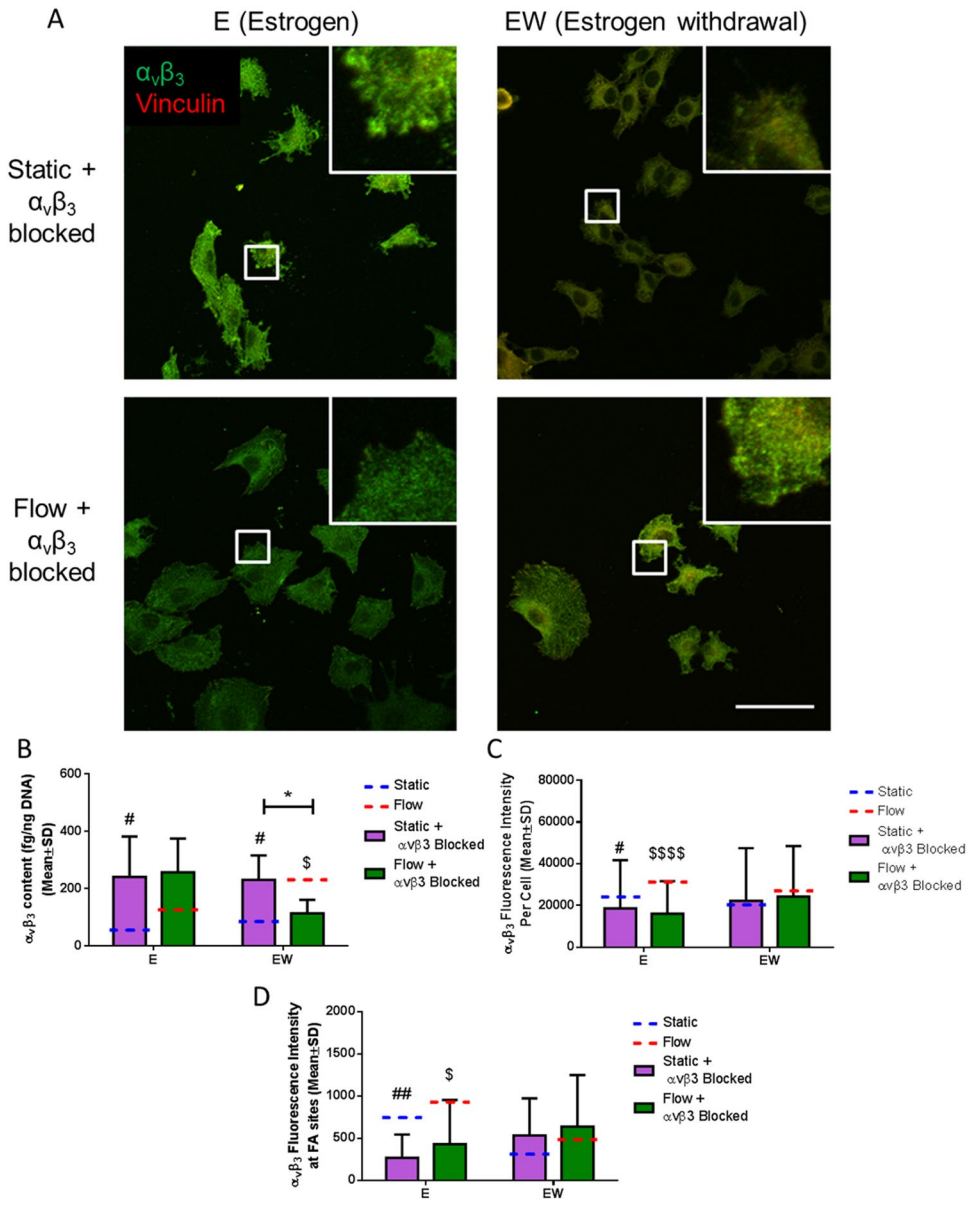

Figure 6. The effect of $\alpha_v\beta_3$ antagonism and oscillatory fluid flow on $\alpha_v\beta_3$ quantity and organisation in MLO-Y4 cells. (**A**) Immunocytochemistry images showing $\alpha_v\beta_3$ and vinculin staining ($N = 3$, $n \geq 90$ cells per group). (**B**) ELISA measurement of total $\alpha_v\beta_3$ quantity normalised to DNA content ($N = 6$). Quantification of the images showing (**C**) $\alpha_v\beta_3$ intensity per cell, and (**D**) $\alpha_v\beta_3$ intensity at focal adhesion (FA) sites (Student's t-test, $^{*}p < 0.05$, $^{\#}p < 0.05$ compared to static, $^{\#\#}p < 0.01$ compared to static, $^{\$}p < 0.05$ compared to flow, $^{\$\$\$\$}p < 0.0001$ compared to flow).

acts a decoy receptor for RANKL[47–51]. It has been established that the application of oscillatory fluid shear stress to MLO-Y4 cells results in a decrease in the *Rankl*/*Opg* ratio[16], which indicates that mechanically stimulated osteocytes reduce paracrine signalling of osteoclastogenesis. We showed that estrogen withdrawal led to an increased *Rankl*/*Opg* ratio. Estrogen withdrawal has been shown to induce osteocyte apoptosis[41,52], which, in turn, leads to changes in RANKL expression[53]. Interestingly, it has previously been reported that in osteoblasts, estrogen treatment led to higher *Opg* expression in a dose-dependent manner, compared to untreated control cells[31]. COX-2 is an enzyme that produces prostaglandins to promote inflammation, and expression of the *Cox-2* is upregulated in osteocytes following oscillatory fluid flow[2,16]. Given the importance of *Cox-2* for normal fracture repair[54] and an increased *Rankl*/*Opg* ratio for inducing osteoclast activity[7,9,26], we propose that under estrogen withdrawal, osteocyte signalling would contribute to the increased bone resorption seen in post-menopausal osteoporosis[26,55].

The importance of integrin $\alpha_v\beta_3$ in osteocyte mechanotransduction has been recently demonstrated[15,17], and, in keeping with a previous study[15], our results show that $\alpha_v\beta_3$ antagonism resulted in a smaller cell area. Interestingly, α_v-integrin antagonism in melanoma cells was shown to lead to rearrangement and disassembly of focal adhesion proteins[56] and we propose that integrin antagonism may have a similar effect on focal adhesion in

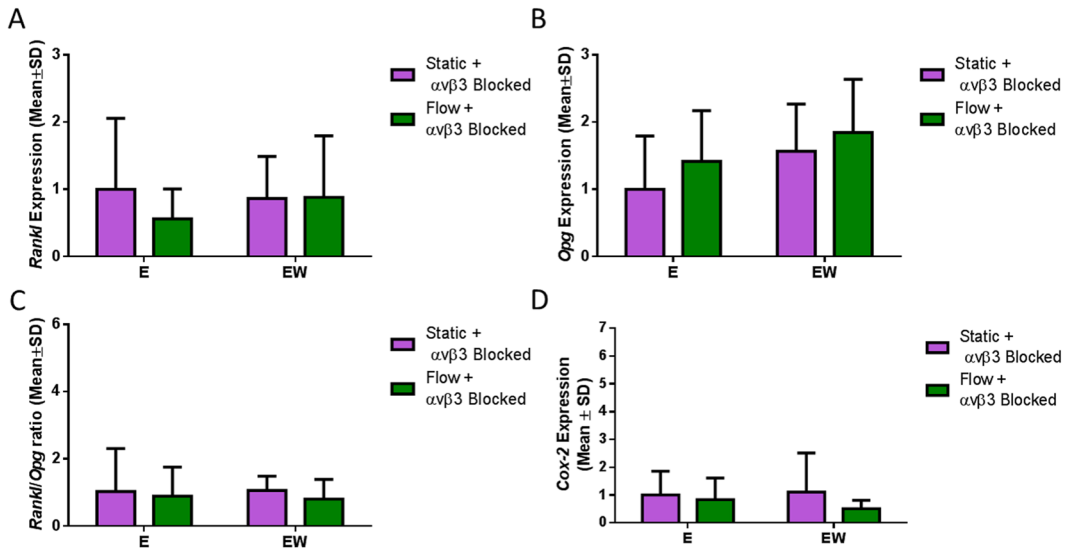

Figure 7. The effect of $\alpha_v\beta_3$ antagonism and oscillatory fluid flow on osteoclastogenic and osteogenic signalling. RT-PCR results of (**A**) *Rankl* expression (N = 6–7), (**B**) *Opg* expression (N = 6–7), (**C**) *Rankl*/*Opg* ratio (N = 4–7) and (**D**) *Cox-2* expression (N = 6–7) (Student's t-test, $^*p < 0.05$).

osteocytes. It is interesting to note that while focal adhesion area was lower following $\alpha_v\beta_3$ antagonism, some distinct focal adhesion sites were present. If we assume that the antagonist blocked all $\alpha_v\beta_3$-containing focal adhesion sites, it is likely that these remaining focal adhesion sites contained other integrin subunits, such as β_1 integrins[4]. $\alpha_v\beta_3$ antagonism resulted in a lower $\alpha_v\beta_3$ fluorescent intensity. Moreover, $\alpha_v\beta_3$ antagonism resulted in an attenuated *Rankl* and *Opg* response following estrogen withdrawal. As the integrin $\alpha_v\beta_3$ was shown to mediate OPG protein production in a human endothelial-breast cancer cell co-culture[57], we propose that the integrin $\alpha_v\beta_3$ plays a similar role in regulating *Rankl* and *Opg* signalling in osteocytes. Previous research studying the role of $\alpha_v\beta_3$ in *Rankl* and *Opg* expression, saw no significant changes following fluid flow, and therefore it was unclear what role the integrin $\alpha_v\beta_3$ played in the *Rankl*/*Opg* response to flow in this instance[15]. Following $\alpha_v\beta_3$ antagonism, we saw a diminished *Cox-2* response to oscillatory fluid flow. Abrogation of this *Cox-2* response to flow following $\alpha_v\beta_3$ antagonism has been demonstrated previously for MLO-Y4 cells cultured under control conditions (no added estrogen)[15]. Other integrin subunits, notably β_1 integrins, play an important role in osteocyte mechanotransduction and have been shown to be necessary for normal *Cox-2* response to flow[16,58]. While the role of β_1 integrins was not investigated in this study, it is interesting to note that β_1 integrins were not fully able to recover *Cox-2* responses to flow following $\alpha_v\beta_3$ antagonism. This may indicate that β_1 and β_3 integrins are closely linked in function *in vitro*. By showing an altered focal adhesion assembly, $\alpha_v\beta_3$ localisation at FA sites, and abrogated *Cox-2* response to flow following estrogen withdrawal or $\alpha_v\beta_3$ antagonism, our study is the first to demonstrate a link between altered osteocyte mechanobiology during estrogen withdrawal and altered $\alpha_v\beta_3$ functionality.

Following mechanical stimulation of osteocytes, $\alpha_v\beta_3$ has been shown to activate MAP kinase pathways leading to an upregulation in c-fos, IGF-1, and *Cox-2*[45]. It has been proposed that upregulation of c-fos is associated with the Ca^{2+} influx pathway[45], which has separately been shown to be mediated by $\alpha_v\beta_3$[17]. In osteoblasts, the $\alpha_v\beta_3$ pathway has been studied more extensively, with the application of fluid flow leading to a synergistic activation of FAK and shc, resulting in the activation of PI3-K and Akt/mTOR/p70S6K pathway, and ultimately increases in *Cox-2* expression[14]. In osteocytes, FAK, PI3-K, and Akt have been shown to be activated in response to fluid shear stress, but it is unknown whether this is mediated by $\alpha_v\beta_3$[59]. Estrogen treatment has been shown to induce FAK phosphorylation, and activation of PI3-K in breast cancer cells[60] and in HUVECs[61]. The breast cancer cells also activated Akt and formed focal adhesion sites in response to estrogen treatment[60]. Thus we propose that *Cox-2* expression by osteocytes following oscillatory fluid flow may arise because $\alpha_v\beta_3$ integrins activate FAK, PI3-K and Akt pathways. Moreover, due to the role of estrogen in regulating FAK and PI3-K pathways in other cell types, we propose that estrogen withdrawal may result in a defect in this proposed $\alpha_v\beta_3$ pathway and could account for the abrogated *Cox-2* response to fluid flow.

There are a number of limitations that must be considered. Firstly, this study involved the use of MLO-Y4 osteocyte-like cells, which were cultured in a monolayer within a parallel plate flow bioreactor. While this cannot fully mimic the mechanical stimulation of osteocytes within the lacunar-canalicular system *in vivo*, both the MLO-Y4 cells and the bioreactor have been used a model extensively *in vitro* to understand the mechanobiology of osteocytes during health and disease[15,16,39,62–64]. Secondly, our regime involved immediate withdrawal of estrogen, but the exact timeline of changes in serum estradiol levels during the menopause *in vivo* is unknown. In humans, serum estradiol levels deplete over a four year period[65], whereas in mice, serum estradiol levels were shown to be lower than normal controls one week after ovariectomy[66]. Thirdly, it was surprising that ELISA measurements of $\alpha_v\beta_3$ antagonism showed a higher $\alpha_v\beta_3$ content compared to unblocked counterparts. We believe that these higher readings may be due to the fact that the $\alpha_v\beta_3$ antagonist was detected by the ELISA along with

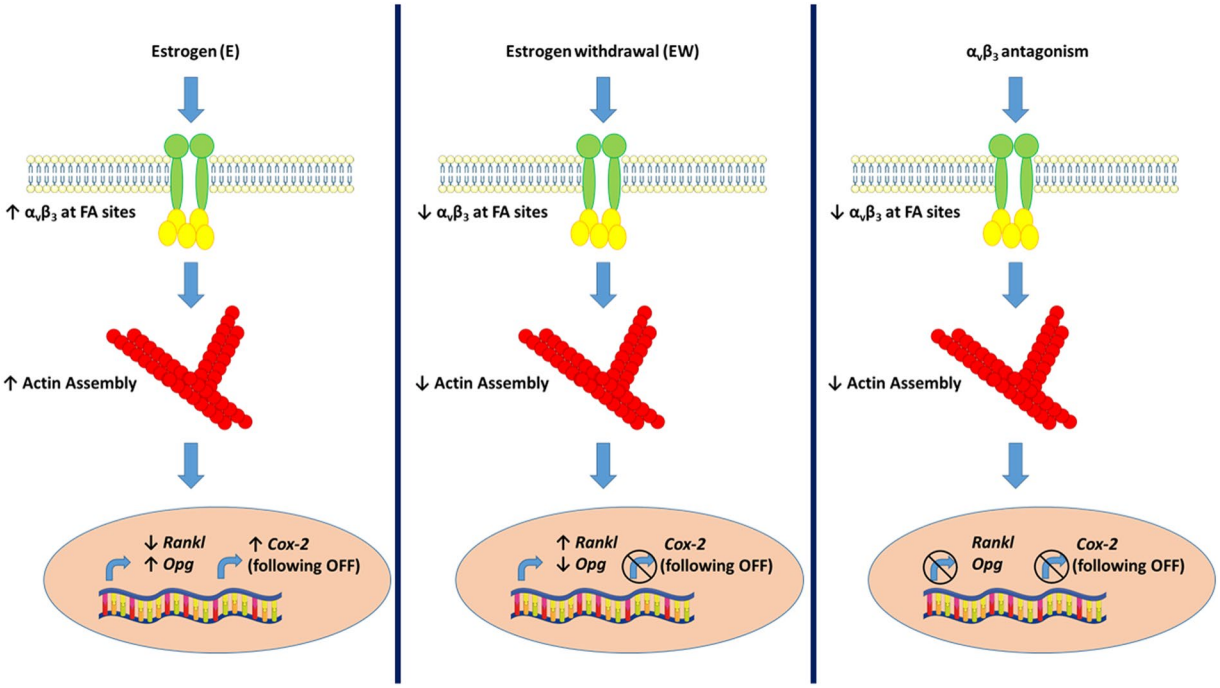

Figure 8. A schematic depicting the effect of estrogen treatment (E), estrogen withdrawal (EW), and $\alpha_v\beta_3$ antagonism.

MLO-Y4 $\alpha_v\beta_3$ integrins. However, it should be noted that the immunocytochemistry staining confirmed the effectiveness of the $\alpha_v\beta_3$ antagonist.

Our results show that the mechanosensor, integrin $\alpha_v\beta_3$, and downstream gene expression is negatively affected by estrogen withdrawal and therefore highlights the importance of integrin $\alpha_v\beta_3$ in post-menopausal osteoporosis. As β_3 integrin expression is affected by estrogen deficiency in OVX animals, this study implicates estrogen withdrawal as the mechanism responsible for altered $\alpha_v\beta_3$ expression and resultant downstream signalling in osteocytes during post-menopausal osteoporosis. Further study to determine a means of protecting the normal expression and signalling of these integrins may offer a potential novel therapy for post-menopausal osteoporosis. Given the altered morphology and gene expression in both estrogen withdrawal conditions and following $\alpha_v\beta_3$ antagonism, it is clear that the integrin $\alpha_v\beta_3$ is affected by estrogen withdrawal and this in turn affects $\alpha_v\beta_3$-mediated signalling. However, it is unlikely that the integrin $\alpha_v\beta_3$ is the only mechanosensor affected by estrogen withdrawal. Many other mechanosensors including β_1 integrins[16], the primary cilium[2], and stretch activated ion channel, TRPV4[3], have all been shown to be important in osteocyte mechanotransduction. To date, the effect of estrogen withdrawal on the ability of these other mechanosensors to transduce mechanical stimulation has not been reported. Given the multitudinous effects of estrogen on cell function, studying the effects of estrogen withdrawal on these other osteocyte mechanosensors may provide an exciting avenue of future research.

Conclusions

Our results show that osteoporotic conditions induced by estrogen withdrawal negatively affected mechanosensor function, specifically through alterations in $\alpha_v\beta_3$ quantity at focal adhesion sites, and that also resulted in impaired mechanobiological responses to flow (*Cox-2* and *Rankl*/*Opg* gene expression). These altered responses to flow were also seen following $\alpha_v\beta_3$ antagonism. We propose that due to the estrogen deficient conditions of post-menopausal osteoporosis, osteocytes undergo altered $\alpha_v\beta_3$ organisation and resultant changes in downstream signalling, particularly those that govern osteoclastogenesis. This research thus uncovers a previously unknown element of the bone loss cascade, whereby estrogen deficiency alters the mechanosensory ability of osteocytes and they in turn contribute to paracrine signalling to govern osteoclast resorption.

Materials and Methods

Cell Culture, and Estrogen Treatment Regimes. MLO-Y4 mouse osteocyte-like cells were cultured on type I collagen (0.15 mg/ml in 0.02 M acetic acid and phosphate buffered saline (PBS)) coated T-75 flasks in α-minimum essential media (α-MEM) supplemented with 5% fetal calf serum (FCS), 5% fetal bovine serum (FBS), 2 mM L-glutamine, 100 U/mL penicillin, and 100 µg/mL streptomycin at 37 °C in a humidified environment at 5% CO_2. The effect of estrogen treatment and estrogen withdrawal on MLO-Y4 cells was studied using the following groups: (1) standard culture media with no added 17β-estradiol (Ctrl), (2) continuous treatment with 10 nM 17 β-estradiol for 5 days (E), and (3) pre-treatment with 10 nM 17β-estradiol for 3 days and withdrawal for 2 further days (EW), following previous approaches developed in our laboratory[39]. On day 3 (two days prior to

the induction of oscillatory fluid flow/static conditions), cells were seeded onto collagen coated glass slides, at a density of 200,000 cells/slide, and cultured for two days in accordance with their treatment groups.

Integrin $\alpha_v\beta_3$ Antagonism. The integrin $\alpha_v\beta_3$ was blocked using a small molecule inhibitor for $\alpha_v\beta_3$ integrins, IntegriSense 750 (PerkinElmer)[15,17]. After removal of culture medium, 1 mL of media containing 0.5 µM IntegriSense 750 was added to each slide for 30 min prior to flow/static conditions. Following this, slides were washed twice with PBS.

Oscillatory Fluid Flow. Laminar oscillatory fluid flow was applied to a cell monolayer using a parallel plate bioreactor system, which consisted of a syringe pump (NE-1600, New Era Pump Systems, Farmingdale, NY), polycarbonate plate chambers, media reservoirs connected by gas-permeable and platinum-cured silicone tubing (Cole-Parmer, Vernon Hills, IL)[15,39]. The fluid flow regime subjected the cell monolayer to a shear stress of 1 Pa at 0.5 Hz for 1 h, which is within the range of shear stresses experiences by osteocytes *in vivo*[25,67–70]. For comparison, static counterparts in each treatment group were not subjected to laminar oscillatory fluid flow conditions for the same time-period.

DNA Content. DNA content was measured using a Hoechst assay. Briefly, 1 mL of sterile deionised (DI) water was carefully placed on each slide and the cells were lysed via the freeze-thaw lysis method in a −80 °C freezer. DNA samples were added to wells with the working dye solution consisting of Hoechst dye: 1X Hoechst Buffer (1:1,000) (Sigma Aldrich). The fluorescence intensity was read using a spectrophotometer for an excitation of 360 nm and at an emission of 460 nm. Calf thymus DNA (Sigma Aldrich) was used as a standard.

Integrin $\alpha_v\beta_3$ Quantification. $\alpha_v\beta_3$ integrin concentration was quantified by means of an $\alpha_v\beta_3$ ELISA (Emelca Bioscience) as per the supplier's protocol. Briefly, cells were lysed used the freeze-thaw lysis method, as above. The sample lysate was placed in the ELISA wells and an antibody against $\alpha_v\beta_3$ was added to each well. Biotin labelled antibodies and horseradish peroxidase were added to further label the samples for $\alpha_v\beta_3$ integrins. The well plate was incubated for 37 °C and washed with a buffer between each of these steps, according to the supplier's protocol. Reagents to aid in colour visualisation were added and the plate absorbance was read at 450 nm using a spectrophotometer (Synergy HT, BioTek). $\alpha_v\beta_3$ integrin concentration readings were normalised to DNA content.

Immunofluorescence. Immunofluorescence was used to study and quantify the spatial distribution of $\alpha_v\beta_3$ integrins in cells from each treatment group cultured statically or following application of flow. Briefly, the cells were washed in PBS and fixed in 3.8% formaldehyde solution, and then permeabilised in 0.1% Triton-X. The cells were incubated in 10% BSA to prevent non-specific binding occurring during the staining process. Integrin $\alpha_v\beta_3$ staining was performed using an anti-$\alpha_v\beta_3$ antibody directly conjugated to Alexa Fluor® 488 (1:100) (Santa Cruz). Vinculin staining was performed using a mouse anti-vinculin primary antibody (1:800) (Sigma Aldrich) and goat anti-mouse Alexa Fluor® 647 secondary antibody (1:200) (Abcam) to label focal adhesion and facilitate the investigation of $\alpha_v\beta_3$ integrin co-localisation (See Supplementary Table 1 for further information on antibodies used). The cells were also stained with TRITC (Tetramethyl Rhodamine Iso-Thiocyanate) Phalloidin and DAPI (4′,6-diamidino-2-phenylindole) to facilitate imaging of the actin cytoskeleton and nucleus respectively. Z-stack imaging was done using a Fluoview FV100 confocal laser scanning microscope system (Olympus) at a magnification of 60x (oil immersion) with a step size of 0.5 µm.

All image analysis was completed using ImageJ software[71]. The z-stacks of the images taken were combined as maximum intensity projections and these combined images were used for all image analysis. Cell area and overall actin fluorescence intensity were measured using the actin stained images. Cell area was measured by thresholding the images to remove background fluorescence and then using the "wand tool" to select the region of interest around each cell. Where two cells were touching, the region of interest was drawn manually with the "freehand tool". Anisotropy of the actin fibrils was determined using a ImageJ plugin, known as FibrilTool[72]. The vinculin stained images were used to identify distinct focal adhesion sites across the entire cell. Identification of distinct focal adhesion sites was enabled by means of a previously published semi-automatic protocol[73]. Focal adhesion area was normalised to cell area. The focal adhesion ROIs thresholded in this process were then used to determine the intensity of the $\alpha_v\beta_3$ staining at focal adhesion sites. All fluorescent intensities were measured using the integrated density of each cell/ROI with their corresponding background integrated density subtracted.

Real Time PCR. Relative gene expression was studied by quantitative Real Time Polymerase Chain Reaction (qRT-PCR). The genes of interest included *Cox-2*, *Rankl*, and *Opg*, with *Rpl13A* used as a reference gene (Supplementary Table 2). RNA was isolated using Qiagen RNeasy kits as per manufacturer's instructions. RNA purity and yield were assessed using a spectrophotometer (DS-11 FX, DeNovix), with 260/280 ratios of >1.9 for all samples. 250–500 ng of RNA was then transcribed into cDNA using Qiagen Quantinova reverse transcription kits and thermal cycler (5PRIMEG/O2, Prime). qRT-PCR was carried out with a Qiagen Quantinova SYBR Green PCR kit and a StepOne Plus PCR machine (Applied Biosciences). Analysis of the results was done using the Pfaffl method[74].

Statistical analysis. Data is presented as mean ± standard deviation. Statistical significance was determined by means of unpaired two-tailed Student's t-tests. All statistical analyses were performed using GraphPad Prism version 6 (Windows, GraphPad Software, La Jolla California USA, www.graphpad.com) and p-value of 0.05.

Data Availability

The datasets generated during and/or analysed during the current study are available from the corresponding author on reasonable request.

References

1. McNamara, L. In *Comprehensive Biomaterials* (eds Ducheyne, P., Healy, K. E., Hutmacher, D. W., Grainger, D. W. & Kirkpatrick, C. J.) 169–186, https://doi.org/10.1016/B978-0-08-055294-1.00068-4 (Elsevier, 2011).
2. Lee, K. L. *et al*. The primary cilium functions as a mechanical and calcium signaling nexus. *Cilia* **4**, 7 (2015).
3. Lyons, J. S. *et al*. Microtubules tune mechanotransduction through NOX2 and TRPV4 to decrease sclerostin abundance in osteocytes. *Sci. Signal.* **10** (2017).
4. McNamara, L. M., Majeska, R. J., Weinbaum, S., Friedrich, V. & Schaffler, M. B. Attachment of osteocyte cell processes to the bone matrix. *Anat Rec* **292**, 355–363 (2009).
5. Lanyon, L. E. Osteocytes, strain detection, bone modeling and remodeling. *Calcif. Tissue Int.* **53** Suppl 1, S102-6; discussionS106-7 (1993).
6. Bonewald, L. F. The amazing osteocyte. *J. Bone Miner. Res.* **26**, 229–238 (2011).
7. Han, Y., You, X., Xing, W., Zhang, Z. & Zou, W. Paracrine and endocrine actions of bone—the functions of secretory proteins from osteoblasts, osteocytes, and osteoclasts. *Bone Res.* **6**, 16 (2018).
8. Li, X. *et al*. Sclerostin Binds to LRP5/6 and Antagonizes Canonical Wnt Signaling. *J. Biol. Chem.* **280**, 19883–19887 (2005).
9. Nakashima, T. *et al*. Evidence for osteocyte regulation of bone homeostasis through RANKL expression. *Nat. Med.* **17**, 1231 (2011).
10. Schaffler, M. B., Cheung, W.-Y., Majeska, R. & Kennedy, O. Osteocytes: Master Orchestrators of Bone. *Calcif. Tissue Int.* **94**, 5–24 (2014).
11. Hughes, D. E., Salter, D. M., Dedhar, S. & Simpson, R. Integrin expression in human bone. *J. Bone Miner. Res.* **8**, 527–533 (1993).
12. Zaidel-Bar, R., Cohen, M., Addadi, L. & Geiger, B. Hierarchical assembly of cell–matrix adhesion complexes. *Biochem. Soc. Trans.* **32**, 416 LP–420 (2004).
13. Mitra, S. K., Hanson, D. A. & Schlaepfer, D. D. Focal adhesion kinase: in command and control of cell motility. *Nat. Rev. Mol. Cell Biol.* **6**, 56 (2005).
14. Lee, D.-Y. *et al*. Oscillatory Flow-induced Proliferation of Osteoblast-like Cells Is Mediated by αvβ3 and β1 Integrins through Synergistic Interactions of Focal Adhesion Kinase and Shc with Phosphatidylinositol 3-Kinase and the Akt/mTOR/p70S6K Pathway. *J. Biol. Chem.* **285**, 30–42 (2010).
15. Haugh, M. G., Vaughan, T. J. & McNamara, L. M. The role of integrin alpha(V)beta(3) in osteocyte mechanotransduction. *J Mech Behav Biomed Mater* **42**, 67–75 (2015).
16. Litzenberger, J. B., Kim, J. B., Tummala, P. & Jacobs, C. R. Beta1 integrins mediate mechanosensitive signaling pathways in osteocytes. *Calcif Tissue Int* **86**, 325–332 (2010).
17. Thi, M. M., Suadicani, S. O., Schaffler, M. B., Weinbaum, S. & Spray, D. C. Mechanosensory responses of osteocytes to physiological forces occur along processes and not cell body and require alphaVbeta3 integrin. *Proc Natl Acad Sci USA* **110**, 21012–21017 (2013).
18. le Duc, Q. *et al*. Vinculin potentiates E-cadherin mechanosensing and is recruited to actin-anchored sites within adherens junctions in a myosin II–dependent manner. *J. Cell Biol.* **189**, 1107–1115 (2003).
19. Yao, M. *et al*. The mechanical response of talin. *Nat. Commun.* **7**, 11966 (2016).
20. Le, S. *et al*. Mechanotransmission and Mechanosensing of Human alpha-Actinin 1. *Cell Rep.* **21**, 2714–2723 (2017).
21. von Wichert, G. *et al*. RPTP-α acts as a transducer of mechanical force on αvβ3-integrin–cytoskeleton linkages. *J. Cell Biol.* **161**, 143 LP–153 (2003).
22. Cabahug-Zuckerman, P. *et al*. Potential role for a specialized β3 integrin-based structure on osteocyte processes in bone mechanosensation. *J. Orthop. Res.* **36**, 642–652 (2017).
23. You, L.-D., Weinbaum, S., Cowin, S. C. & Schaffler, M. B. Ultrastructure of the osteocyte process and its pericellular matrix. *Anat. Rec. Part A Discov. Mol. Cell. Evol. Biol.* **278A**, 505–513 (2004).
24. You, L., Cowin, S. C., Schaffler, M. B. & Weinbaum, S. A model for strain amplification in the actin cytoskeleton of osteocytes due to fluid drag on pericellular matrix. *J. Biomech.* **34**, 1375–1386 (2001).
25. Wang, Y., McNamara, L. M., Schaffler, M. B. & Weinbaum, S. A model for the role of integrins in flow induced mechanotransduction in osteocytes. *Proc Natl Acad Sci USA* **104**, 15941–15946 (2007).
26. McNamara, L. M. Perspective on post-menopausal osteoporosis: establishing an interdisciplinary understanding of the sequence of events from the molecular level to whole bone fractures. *J R Soc Interface* **7**, 353–372 (2010).
27. Krum, S. A. *et al*. Estrogen protects bone by inducing Fas ligand in osteoblasts to regulate osteoclast survival. *EMBO J.* **27**, 535–545 (2008).
28. Bakker, A. D. *et al*. Additive effects of estrogen and mechanical stress on nitric oxide and prostaglandin E2 production by bone cells from osteoporotic donors. *Osteoporos. Int.* **16**, 983–989 (2005).
29. Zaman, G. *et al*. Osteocytes Use Estrogen Receptor α to Respond to Strain but Their ERα Content Is Regulated by Estrogen. *J. Bone Miner. Res.* **21**, 1297–1306 (2009).
30. Castillo, A. B., Triplett, J. W., Pavalko, F. M. & Turner, C. H. Estrogen receptor-β regulates mechanical signaling in primary osteoblasts. *Am. J. Physiol. - Endocrinol. Metab.* **306**, E937–E944 (2014).
31. Jia, J., Zhou, H., Zeng, X. & Feng, S. Estrogen stimulates osteoprotegerin expression via the suppression of miR-145 expression in MG-63 cells. *Mol. Med. Rep.* **15**, 1539–1546 (2017).
32. Yeh, C.-R. *et al*. Estrogen Augments Shear Stress–Induced Signaling and Gene Expression in Osteoblast-like Cells via Estrogen Receptor–Mediated Expression of β(1)-Integrin. *J. Bone Miner. Res.* **25**, 627–639 (2010).
33. Galea, G. L. *et al*. Estrogen Receptor α Mediates Proliferation of Osteoblastic Cells Stimulated by Estrogen and Mechanical Strain, but Their Acute Down-regulation of the Wnt Antagonist Sost Is Mediated by Estrogen Receptor β. *J. Biol. Chem.* **288**, 9035–9048 (2013).
34. Bord, S., Ireland, D. C., Beavan, S. R. & Compston, J. E. The effects of estrogen on osteoprotegerin, RANKL, and estrogen receptor expression in human osteoblasts. *Bone* **32**, 136–141 (2003).
35. Marathe, N., Rangaswami, H., Zhuang, S., Boss, G. R. & Pilz, R. B. Pro-survival Effects of 17β-Estradiol on Osteocytes Are Mediated by Nitric Oxide/cGMP via Differential Actions of cGMP-dependent Protein Kinases I and II. *J. Biol. Chem.* **287**, 978–988 (2012).
36. Plotkin, L. I., Aguirre, J. I., Kousteni, S., Manolagas, S. C. & Bellido, T. Bisphosphonates and Estrogens Inhibit Osteocyte Apoptosis via Distinct Molecular Mechanisms Downstream of Extracellular Signal-regulated Kinase Activation. *J. Biol. Chem.* **280**, 7317–7325 (2005).
37. Ren, J. & Wu, J. H. 17β-Estradiol Rapidly Activates Calcium Release from Intracellular Stores via the GPR30 Pathway and MAPK Phosphorylation in Osteocyte-Like MLO-Y4 Cells. *Calcif. Tissue Int.* **90**, 411–419 (2012).
38. Ren, J., Wang, X.-H., Wang, G.-C. & Wu, J.-H. 17β Estradiol regulation of connexin 43-based gap junction and mechanosensitivity through classical estrogen receptor pathway in osteocyte-like MLO-Y4 cells. *Bone* **53**, 587–596 (2013).
39. Deepak, V., Kayastha, P. & McNamara, L. M. Estrogen deficiency attenuates fluid flow–induced [Ca2+]i oscillations and mechanoresponsiveness of MLO-Y4 osteocytes. *FASEB J.*, https://doi.org/10.1096/fj.201601280R (2017).

40. Sterck, J. G. H., Klein-Nulend, J., Lips, P. & Burger, E. H. Response of normal and osteoporotic human bone cells to mechanical stress *in vitro*. *Am. J. Physiol. - Endocrinol. Metab.* **274**, E1113 LP–E1120 (1998).
41. Brennan, M. A. *et al*. Estrogen Withdrawal from Osteoblasts and Osteocytes Causes Increased Mineralization and Apoptosis. *Horm. Metab. Res.* **46**, 537–545 (2014).
42. Voisin, M. & McNamara, L. M. Differential β_3 and β_1 Integrin Expression in Bone Marrow and Cortical Bone of Estrogen Deficient Rats. *Anat. Rec.* **298**, 1548–1559 (2015).
43. Verbruggen, S. W. W., Mc Garrigle, M. J. J., Haugh, M. G. G., Voisin, M. C. C. & McNamara, L. M. M. Altered Mechanical Environment of Bone Cells in an Animal Model of Short- and Long-Term Osteoporosis. *Biophys. J.* **108**, 1587–1598 (2015).
44. Brennan, M. A., Gleeson, J. P., O'Brien, F. J. & McNamara, L. M. Effects of ageing, prolonged estrogen deficiency and zoledronate on bone tissue mineral distribution. *J. Mech. Behav. Biomed. Mater.* **29**, 161–170 (2014).
45. Miyauchi, A. *et al*. AlphaVbeta3 integrin ligands enhance volume-sensitive calcium influx in mechanically stretched osteocytes. *J Bone Min. Metab* **24**, 498–504 (2006).
46. Vaughan, T. J., Mullen, C. A., Verbruggen, S. W. & McNamara, L. M. Bone cell mechanosensation of fluid flow stimulation: a fluid–structure interaction model characterising the role integrin attachments and primary cilia. *Biomech. Model. Mechanobiol.* **14**, 703–718 (2015).
47. Clarke, B. Normal Bone Anatomy and Physiology. *Clin. J. Am. Soc. Nephrol.* **3**, S131 LP–S139 (2008).
48. Boyce, B. F. & Xing, L. Functions of RANKL/RANK/OPG in bone modeling and remodeling. *Arch. Biochem. Biophys.* **473**, 139–146 (2008).
49. Yasuda, H. *et al*. Osteoclast differentiation factor is a ligand for osteoprotegerin/osteoclastogenesis-inhibitory factor and is identical to TRANCE/RANKL. *Proc. Natl. Acad. Sci.* **95**, 3597 LP–3602 (1998).
50. Asagiri, M. & Takayanagi, H. The molecular understanding of osteoclast differentiation. *Bone* **40**, 251–264 (2007).
51. Takayanagi, H. The Role of NFAT in Osteoclast Formation. *Ann. N. Y. Acad. Sci.* **1116**, 227–237 (2007).
52. Emerton, K. B. *et al*. Osteocyte apoptosis and control of bone resorption following ovariectomy in mice. *Bone* **46**, 577–583 (2010).
53. Cabahug-Zuckerman, P. *et al*. Osteocyte Apoptosis Caused by Hindlimb Unloading is Required to Trigger Osteocyte RANKL Production and Subsequent Resorption of Cortical and Trabecular Bone in Mice Femurs. *J. Bone Miner. Res.* **31**, 1356–1365 (2016).
54. Forwood, M. R. Inducible cyclo-oxygenase (COX-2) mediates the induction of bone formation by mechanical loading *in vivo*. *J. Bone Miner. Res.* **11**, 1688–1693 (1996).
55. Brennan, O. *et al*. Temporal changes in bone composition, architecture, and strength following estrogen deficiency in osteoporosis. *Calcif Tissue Int* **91**, 440–449 (2012).
56. Castel, S. *et al*. Alpha v integrin antagonists induce the disassembly of focal contacts in melanoma cells. *Eur. J. Cell Biol.* **79**, 502–512 (2000).
57. Reid, P. E., Brown, N. J. & Holen, I. Breast cancer cells stimulate osteoprotegerin (OPG) production by endothelial cells through direct cell contact. *Mol. Cancer* **8**, 49 (2009).
58. Litzenberger, J. B., Tang, W. J., Castillo, A. B. & Jacobs, C. R. Deletion of β1 Integrins from Cortical Osteocytes Reduces Load-Induced Bone Formation. *Cell. Mol. Bioeng.* **2**, 416–424 (2009).
59. Santos, A., Bakker, A. D., Zandieh-Doulabi, B., de Blieck-Hogervorst, J. M. A. & Klein-Nulend, J. Early activation of the β-catenin pathway in osteocytes is mediated by nitric oxide, phosphatidyl inositol-3 kinase/Akt, and focal adhesion kinase. *Biochem. Biophys. Res. Commun.* **391**, 364–369 (2010).
60. Sanchez, A. M. *et al*. Estrogen Receptor-α Promotes Breast Cancer Cell Motility and Invasion via Focal Adhesion Kinase and N-WASP. *Mol. Endocrinol.* **24**, 2114–2125 (2010).
61. Sanchez, A. M. *et al*. Estrogen receptor-α promotes endothelial cell motility through focal adhesion kinase. *MHR Basic Sci. Reprod. Med.* **17**, 219–226 (2011).
62. Alford, A. I., Jacobs, C. R. & Donahue, H. J. Oscillating fluid flow regulates gap junction communication in osteocytic MLO-Y4 cells by an ERK1/2 MAP kinase-dependent mechanism small star, filled. *Bone* **33**, 64–70 (2003).
63. Cheng, B. *et al*. Expression of functional gap junctions and regulation by fluid flow in osteocyte-like MLO-Y4 cells. *J. Bone Miner. Res.* **16**, 249–259 (2001).
64. Vaughan, T. J., Haugh, M. G. & McNamara, L. M. A fluid-structure interaction model to characterize bone cell stimulation in parallel-plate flow chamber systems. *J. R. Soc. Interface* **10**, 20120900 (2013).
65. Sowers, M. R. *et al*. Estradiol Rates of Change in Relation to the Final Menstrual Period in a Population-Based Cohort of Women. *J. Clin. Endocrinol. Metab.* **93**, 3847–3852 (2008).
66. Smeester, B., *et al The relationship of bone-tumor induced spinal cord astrocyte activation and aromatase expression to mechanical hyperalgesia and cold hypersensitivity in intact female and ovariectomized mice*. *Neuroscience* **324** (2016).
67. Han, Y., Cowin, S. C., Schaffler, M. B. & Weinbaum, S. Mechanotransduction and strain amplification in osteocyte cell processes. *Proc. Natl. Acad. Sci. USA* **101**, 16689–16694 (2004).
68. Verbruggen, S. W., Vaughan, T. J. & McNamara, L. M. Strain amplification in bone mechanobiology: a computational investigation of the *in vivo* mechanics of osteocytes. *J. R. Soc. Interface* **9**, 2735–44 (2012).
69. Weinbaum, S., Cowin, S. C. & Zeng, Y. A model for the excitation of osteocytes by mechanical loading-induced bone fluid shear stresses. *J. Biomech.* **27**, 339–360 (1994).
70. Li, J., Rose, E., Frances, D., Sun, Y. & You, L. Effect of oscillating fluid flow stimulation on osteocyte mRNA expression. *J. Biomech.* **45**, 247–251 (2012).
71. Schneider, C. A., Rasband, W. S. & Eliceiri, K. W. NIH Image to ImageJ: 25 years of image analysis. *Nat. Methods* **9**, 671 (2012).
72. Boudaoud, A. *et al*. FibrilTool, an ImageJ plug-in to quantify fibrillar structures in raw microscopy images. *Nat. Protoc.* **9**, 457 (2014).
73. Horzum, U., Ozdil, B. & Pesen-Okvur, D. Step-by-step quantitative analysis of focal adhesions. *MethodsX* **1**, 56–59 (2014).
74. Pfaffl, M. W. A new mathematical model for relative quantification in real-time RT–PCR. *Nucleic Acids Res.* **29**, e45–e45 (2001).

Acknowledgements

This publication has emanated from research conducted with the financial support of Science Foundation Ireland (SFI) and is co-funded under the European Regional Development Fund under Grant Number 13/RC/2073 and Grant Number 14/IA/2884. The authors acknowledge funding from European Research Council (ERC) Starting Grant (336882) and Science Foundation Ireland (SFI) Grants 13/ERC/L2864 and 12/RC/2278. The MLO-Y4 cell line used in this study was received as a kind gift from Professor Lynda Bonewald (School of Dentistry, University of Missouri, Kansas City, MO, U.S.A.). The authors acknowledge the facilities and scientific and technical assistance of the Centre for Microscopy & Imaging at the National University of Ireland Galway (www.imaging.nuigalway.ie). The authors acknowledge the facilities and scientific and technical assistance of the Genomics and Screening Core at the National University of Ireland Galway, a facility that is funded by NUIG and the Irish Government's Programme for Research in Third Level Institutions, Cycles 4 and 5, National Development Plan 2007–2013.

Author Contributions

I.G. designed and performed experiments, interpreted the data, and wrote the manuscript; D.A.H. designed experiments, interpreted the data, and wrote the manuscript; and L.M.M. designed experiments, interpreted the data, and wrote the manuscript.

Additional Information

Supplementary information accompanies this paper at https://doi.org/10.1038/s41598-019-41095-3.

Competing Interests: The authors declare no competing interests.

Publisher's note: Springer Nature remains neutral with regard to jurisdictional claims in published maps and institutional affiliations.